P-wave tomography and deep structure of the cross sections :

Local earthquake tomography (LET) results by Diehl et al. (2009) document the average P wave velocity – averaged over the volume of each cell. Based on the pronounced and systematic velocity increase across the crust-mantle boundary, Moho topography may unambiguously be derived from LET results (Wagner et al. 2012). Moho depths are based on combined controlled-source seismology, local earthquake tomography and receiver function data evaluated individually for their uncertainties and compiled in a procedure outlined in details in Wagner et al. 2012 and Spada et al. 2013. Within the crust, however, absolute P velocities and lateral and vertical velocity variations in LET are less conclusive since various lithologies might contribute to the single cell average and since different lithologies exhibit similar velocities. As a first-order approximation and in the case of more or less horizontally layered normal continental crust one may attribute the 6km/sec iso-velocity contour to the near top granitic basement and the 6.5km/sec iso-velocity contour to the near top lower continental crust. In the structurally complex Alpine cross sections we applied the latter iso-velocity contour to distinguish between mainly upper and lower crustal material. Note that nappes originating from the more distal continental margin may include parts of oceanic crustal material and high pressure rocks, thus exhibiting velocities similar to those of lower continental crust.

Engadine section (Figure 1a):
The 6,5 km/s contour line, shows a complex, almost concentric anomaly across the entire nappe pile of the European plate. This structure, inferred to be robust because it persists along strike for several tens of km in the tomographic models (Diehl et al., 2009), was used to construct the thickening of the lower crust and the eastern termination of the nappes on the European plate.

Bergell section (Figure 1b):
This cross section is taken from Schmid et al. (1996) and it was published long before the existence of the P-wave tomography used in our study (Diehl et al. 2009). For comparison with the other cross section we show the iso-velocity contour lines, but we did not use them to constrain the deep structure of this section.

Simplon section (Figure 1c):
The 6 km/s line, closely shows the double dome structure of the accreted wedge of lower plate material. The 6.5 km/s line marks the transition from the lower crust to the middle crust both in the upper and in the lower plate, showing a step in the contact zone of the two plates, parallel to the steepened, Adriatic mantle. The 7 km/s parallels the Moho in large parts of the section, showing a step toward a highr Moho in the Adriatic plate.

Shortening estimates and restored sections

Engadine section :

Inferred collisional shortening has been taken from previously published studies. For the TALP shortening of 10-12 km were inferred based on restoration of the nappe structure below the Engadine Window, inferred from seismic interpretation (Hitz, 1995). Shortening in the upper Adriatic plate is inferred on the base of balanced cross sections (Schönborn, 1992). The complete restored cross section is shown in Fig. 2b.

Bergell section:
The Aar and Gotthard Massifs form an « excess area » of 373 km^2 compared to the non-thickened European basement underlying the Molasse basin (Fig. **2**). The lower crust of the TALP in this section becomes detached from the mid-crust below the orogen, suggesting a depth of detachment located at the top of the lower crust. In addition, the basal detachments of the Aar massif are inferred to be kinematically linked to the tip of the South-Alpine indenter, hence confirming that the detachment below the Aar Massif needs to be located on top of the lower crust. Restoration of the excess surface on top of such a detachment, corresponds to a shortening of 21 km.
Shortening of 21 km by the Cressim antiform was inferred by line-length balancing of the top of the distal European nappes, assuming that it was lying nearly horizontally, before collision.
The restored lower plate of the Bergell section (Fig. 3b) is modified from Schmid et al. (1996). Restoration of the upper plate is from (Schönborn, 1992).

Simplon section :
The Aar and Gotthard Massifs form an « excess area » of 560 km^2 compared to the non-thickened European basement underlying the Molasse basin (Fig. 4**)**. The Simplon cross section shows that the lower crust of the TALP becomes detached from the mid-crust below the orogen, suggesting a depth of detachment at the top of the lower crust. In addition, the basal detachments of the Aar massif are inferred to be kinematically linked to the tip of the South-Alpine indenter (in this case the tip of the Ivrea Mantle), hence confirming that the detachment below the Aar Massif needs to be located on top of the lower crust. Restoration of the excess surface on top of such a detachment, corresponds to a shortening of 34 km. This value is smaller than the one inferred by Kempf and Pfiffner (2004).
Shortening of 37 km by the Vanzone antiform was inferred by line-length balancing of the top of the distal European nappes, assuming that it was lying nearly horizontally, before collision. Shortening in the upper plate was taken from Schumacher et al. (1997). The complete restored cross section is shown in Fig. 4b.
Deep rooting of the Briançonnais and Austroalpine Units in this section is a geometrical necessity, constrained by surface geology (subvertically dipping in the Southern Steep Belt » and it is also consistent with both the other sections, where it is also observable from surface geological data that the Austroalpine must be deeply rooted within the nappe stack.

Figure Captions

Fig. DR1 : Pk wave tomography of the Engadin, the Bergell, and the Simplon sections.

Fig. DR2 : Engadine section. 2a) Presentk day. 2b) Section restored to 31.5 Ma.

Fig. DR3 : Bergell section. 3a) Presentk day. 3b) Section restored to 31.5 Ma.

Fig. DR4 : Simplon section. 4a) Presentk day. 4b) Section restored to 31.5 Ma.

References:

Diehl, T., Husen, S., Kissling, E., and Deichmann, N., 2009, High-resolution 3-D P-wave model of the Alpine crust. Geophysical Journal International, 179, 1133–1147.

Escher, A., Masson, H., and Steck, A., 1993, Nappe geometry in the Western Swiss Alps. Journal of Structural Geology, 15, 501-509.

Freitag U., Kley, J., Gaupp, R., and Adelmann, D., 2004, Balanced structural cross-section across the northern margin of the Alps (Southern Germany) between the wells Legau and HindelangAbstract, AAPG European Region Conference, Prague, Czech Republic.

Hitz, L., 1995, The 3D crustal structure of the Alps of eastern Switzerland and western Austria interpreted from a network of deep-seismic profiles. Tectonophysics, 248, 71-96

Lombardi, D. , J. Braunmiller, E. Kissling and D. Giardini, 2012, Moho depth and poisson's ratio in the western-central alps from receiver functions. Geophys. J. Int.

Kempf, O., and Pfiffner, A.O., 2004, Early Tertiary evolution of the North Alpine Foreland Basin of the Swiss Alps and adjoining areas. Basin Research, 16, 549–567.

Pieri M. e Groppi G.; 1981: Subsurface geological structure of the Po Plain (Italy). C.N.R., Prog. Fin. Geod., n. 414, 1-13.

Schmid, S., Pfiffner, 0. A., Froitzheim, N., Schönborn, G., and Kissling, E., (1996),

Geophysical-geological transect and tectonic evolution of the Swiss-Italian Alps, Tectonics, 15, 1036 – 1064.

Schmid, S. M., and E. Kissling (2000), The arc of the Western Alps in the light of geophysical data on deep crustal structure, Tectonics, 19, 62 – 85.

Schönborn, G. (1992), Alpine tectonics and kinematic models of the central southern Alps, Mem. Sci. Geol. Padova, 44, 229 – 293.

Spillmann, P., 1993, Die Geologie des penninisch-ostalpinen Grenzbereichs im südlichen Berninagebirge. PhD, ETH Zuerich, Nr. 10175.

Steck, A., Epard, J.-L., Escher, A., Gouffon, Y., and Masson, H., 2001, Carte tectonique des Alpes de Suisse occidentale et des regions avoisinantes 1:100.000. Notice explicative. Vol. 123 of Geologische Spezialkarte. Office federal des eaux et de la géologie.

Wagner, M., Kissling, E. and Husen, S., 2012. Combining controlled-source seismology and local earthquake tomography to derive a 3-D crustal model of the western Alpine region. Geophysical Journal International, 191, 789–802 .

P-wave tomography of Engadine section, extracted from Diehl et al. (2009) and Wagner et al. (2012).

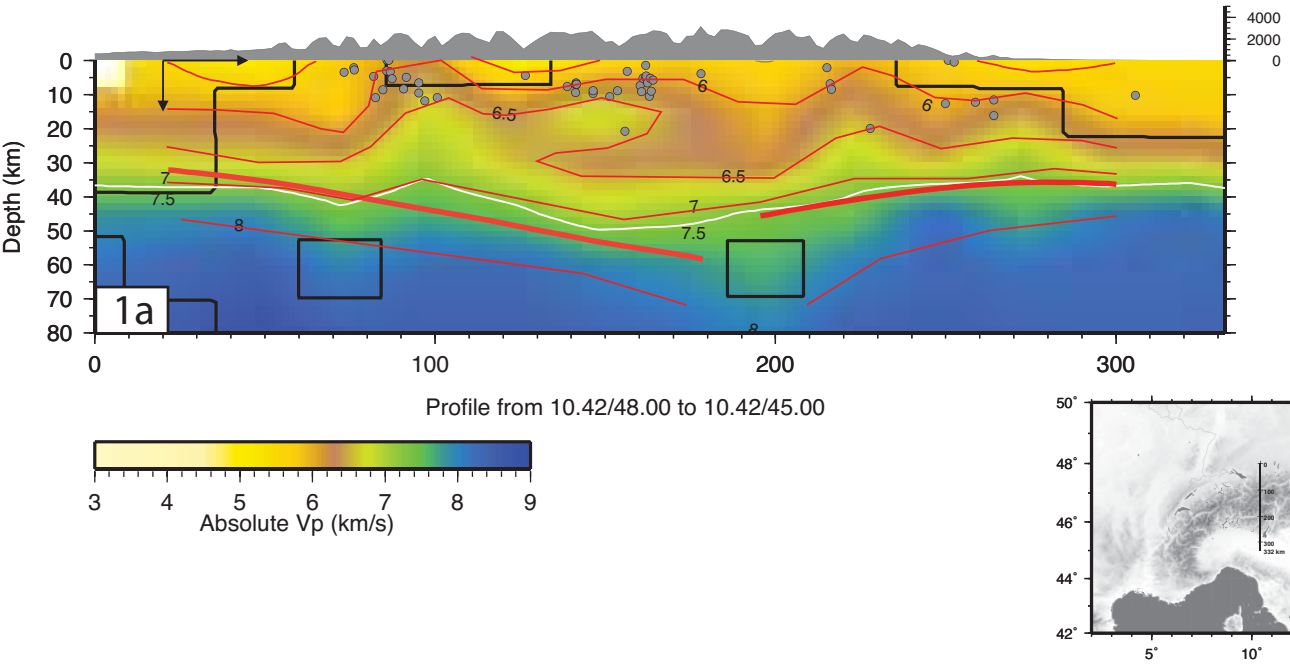

P-wave tomography of Bergell section, extracted from Diehl et al. (2009) and Wagner et al. (2012).

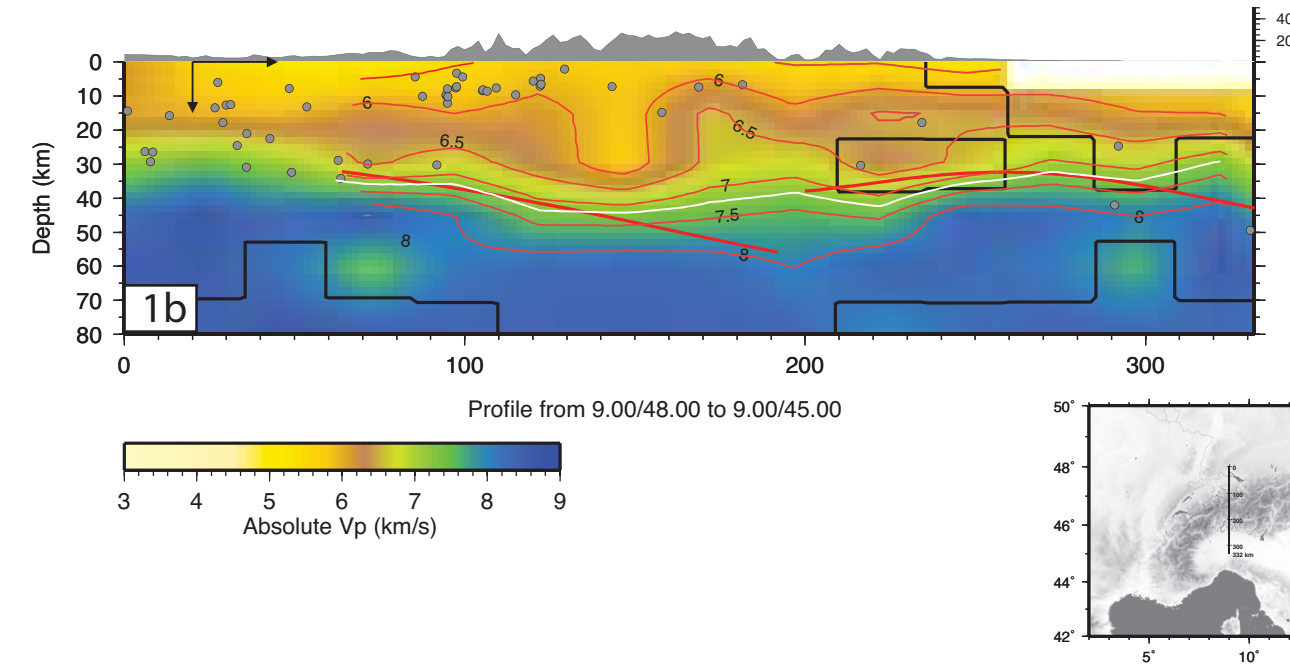

P-wave tomography of Simplon section, extracted from Diehl et al. (2009) and Wagner et al. (2012).

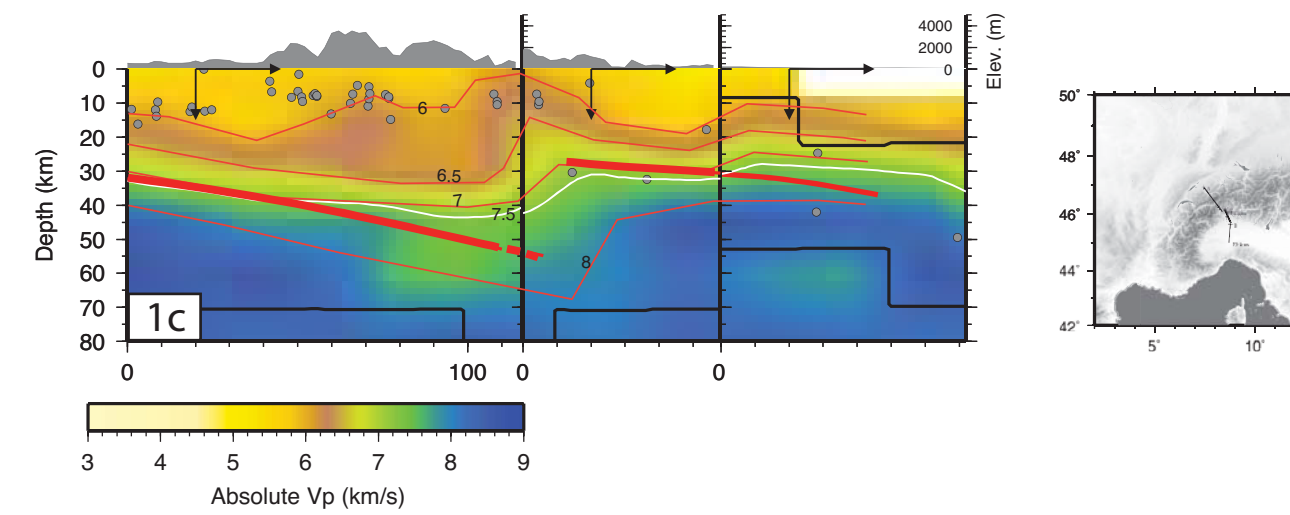

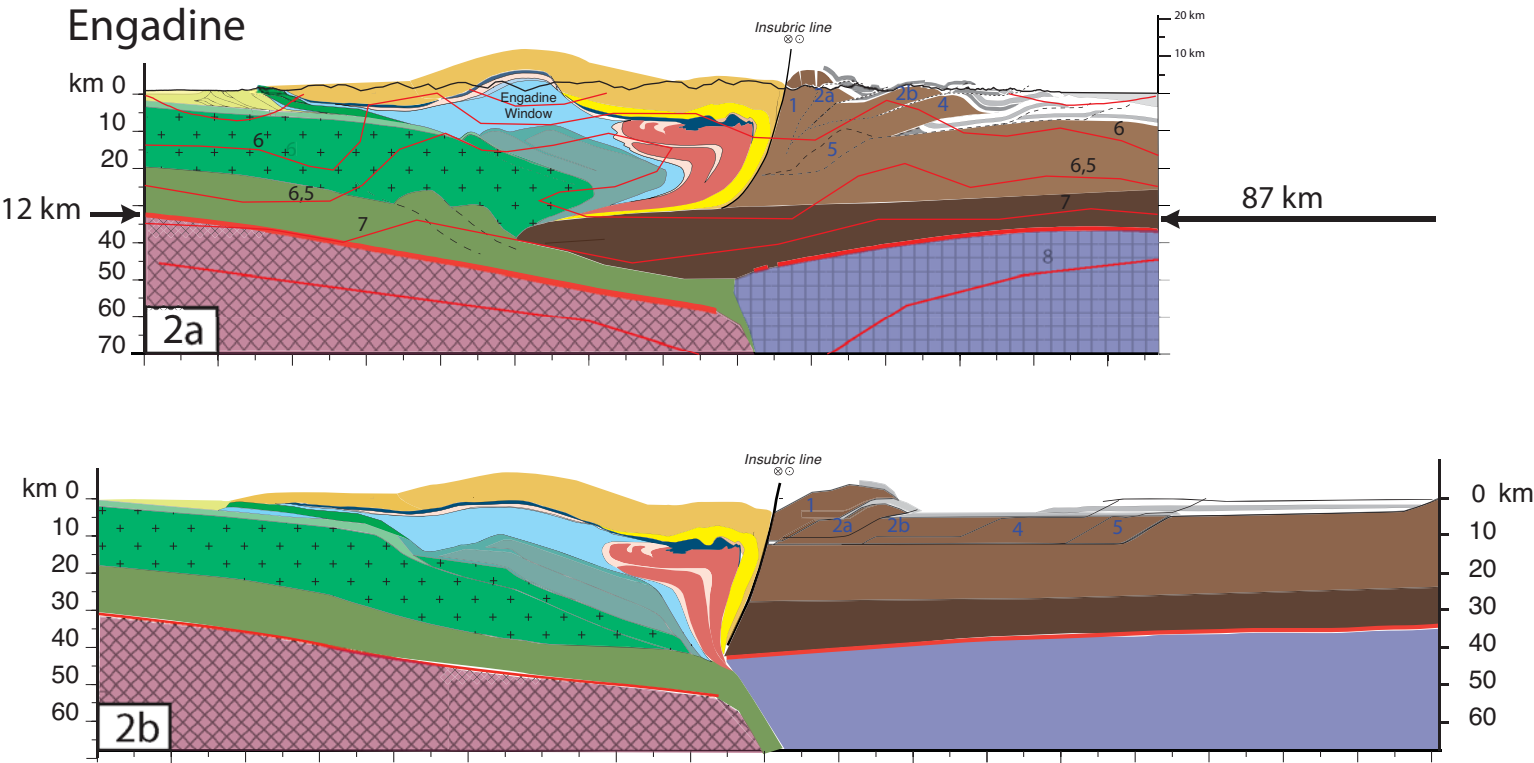
Engadine
Insubric line
20 km
10 km
km 0
10
20
12 km
40
50
60
70
Engadine Window
1
2a
2b
4
5
6
6,5
7
8
87 km
2a
Insubric line
km 0
10
20
30
40
50
60
0 km
10
20
30
40
50
60
2a
2b
4
5
2b

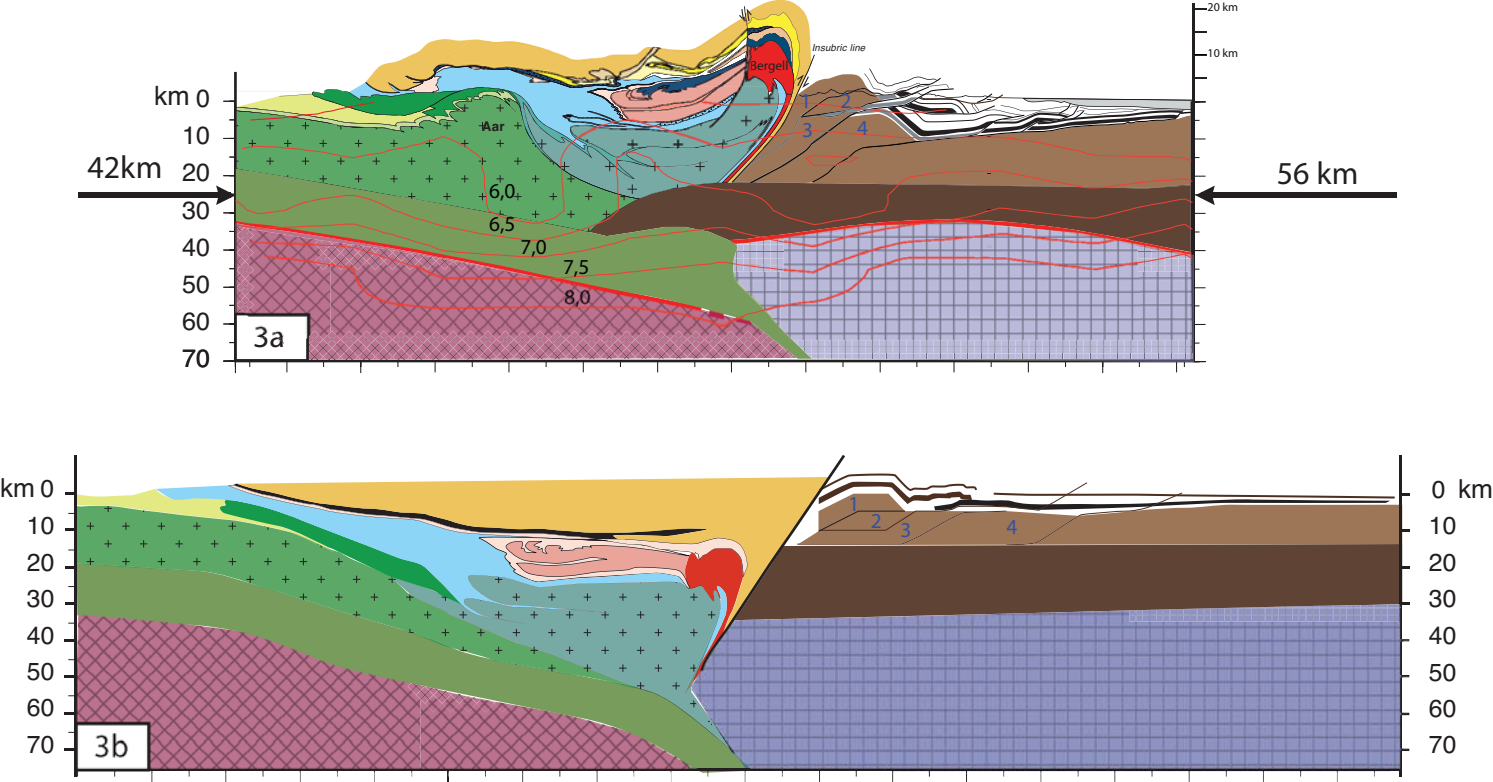
20 km
10 km
Insubric line
Bergell
km 0
10
20
30
40
50
60
70
Aar
42km
56 km
6,0
6,5
7,0
7,5
8,0
1
2
3
4
3a
km 0
10
20
30
40
50
60
70
0 km
10
20
30
40
50
60
70
1
2
3
4
3b

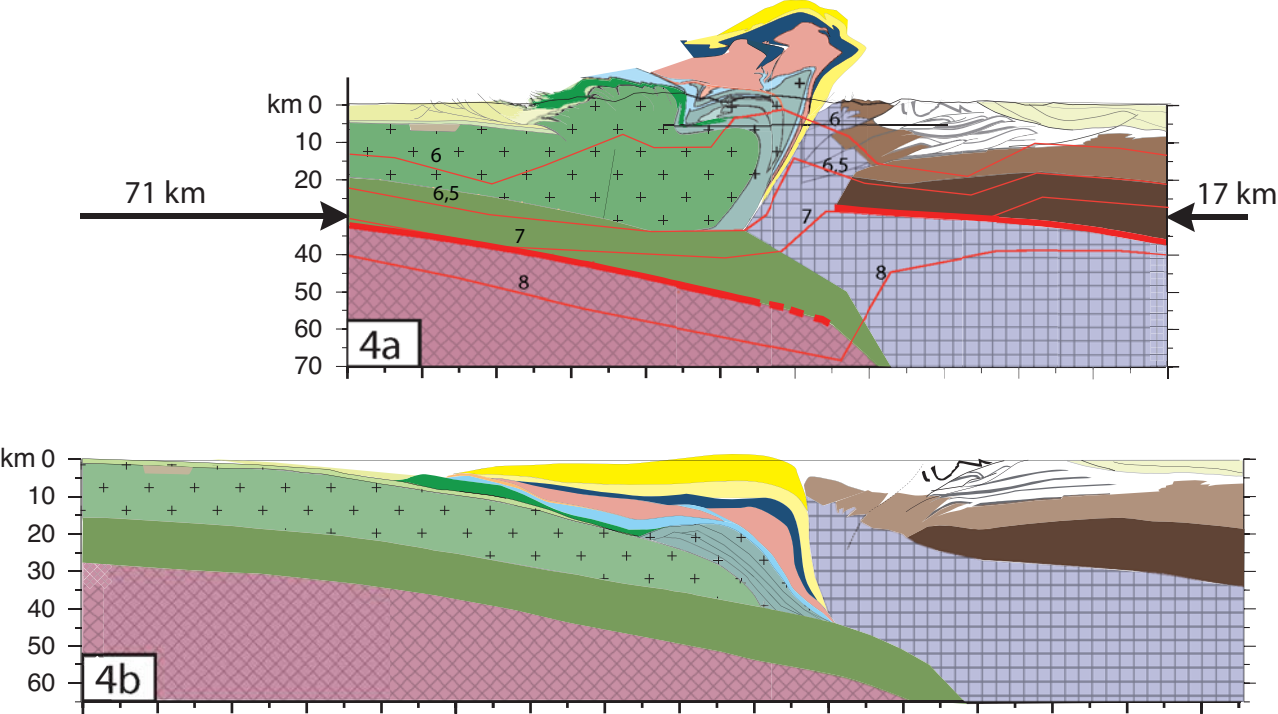
km 0
10
20
30
40
50
60
70
71 km
17 km
6
6,5
7
8
4a
4b